

# TUNGSTEN ION DATA NEEDS AND TUNGSTEN SPECTRAL DATA COMPILATION AT NIFS

I. Murakami<sup>1,2</sup>, D. Kato<sup>1,3</sup>

<sup>1</sup> National Institute for Fusion Science, Toki, Gifu, 509-5292,  
Japan

<sup>2</sup> Graduate Institute for Advanced Studies, SOKENDAI, Toki,  
Gifu, 509-5292, Japan

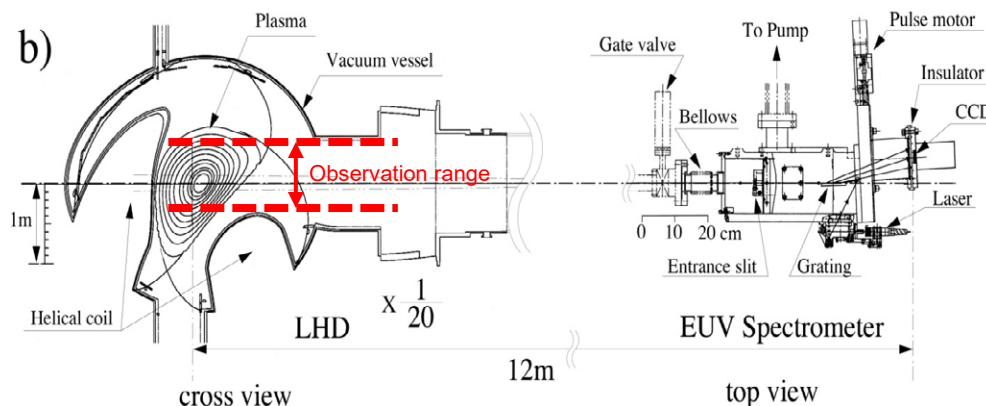
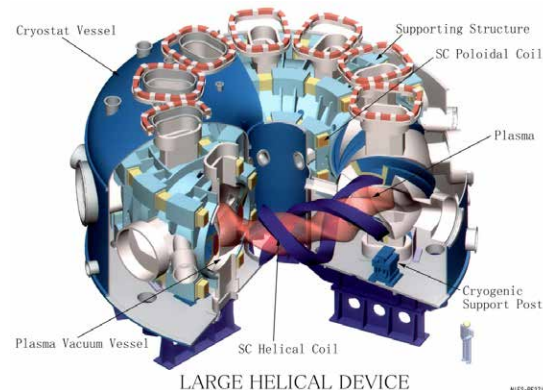
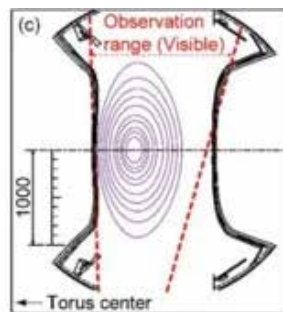
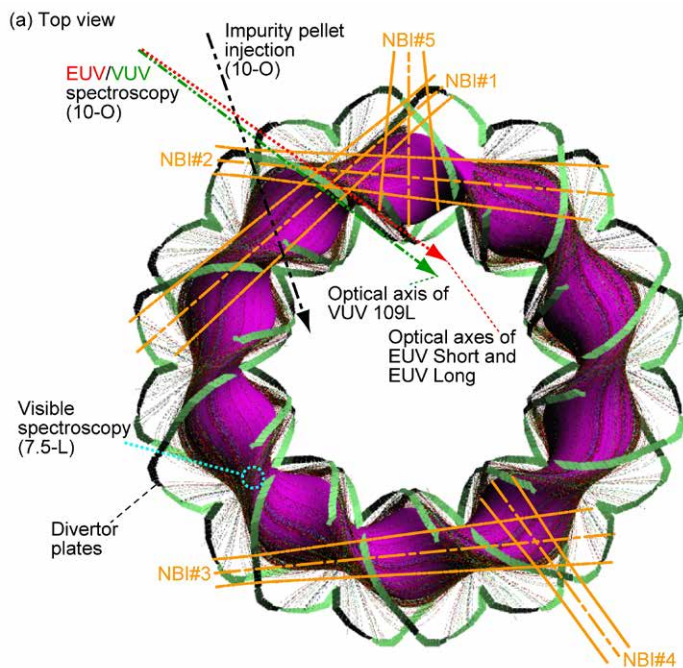
<sup>3</sup> Interdisciplinary Graduate School of Engineering Sciences,  
Kyushu University, Kasuga 816-8580, Japan

# 1. Introduction

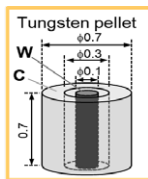
- In order to understand tungsten impurity behavior in magnetically confined plasmas, we have measured tungsten ion spectra from soft X-ray to visible wavelength regions for LHD plasmas with tungsten pellet injection.
- LHD plasma is stable with impurity injection and tungsten are transported and accumulated at the core region under a certain condition.
- Accumulated tungsten ions reduce electron temperature at the core due to large radiation power and temperature hole structure is achieved. Continuous NBI heating helps to recover electron temperature. According to the electron temperature change, charge states of tungsten ion change.
- We have constructed collisional-radiative models for tungsten ions,  $W^{q+}$  with  $q=5, 13, 20-39$ , and  $44$ , with atomic data calculated with HULLAC code to compare with measured spectra.

# 2. W spectral measurement in Large Helical Device (LHD)

- LHD at NIFS is suitable to measure tungsten spectra because it is stable with impurity injection and bright to measure spectra from Soft X-ray to visible wavelength ranges.



Tungsten impurity is introduced by an impurity pellet or a TESPEL injection.



## Impurity pellet

W wire in a C pellet:  
 $l 0.7 \text{ mm} \times \phi 0.1 \text{ mm}$   
 $\sim 3.5 \times 10^{17} \text{ W atoms}$

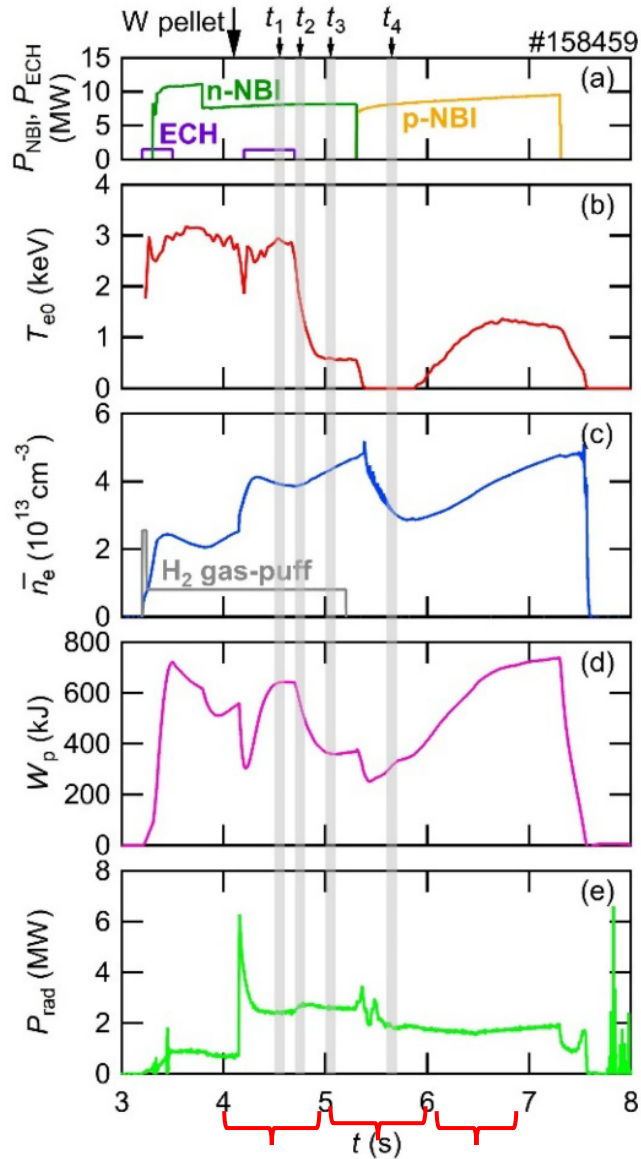


TESPEL  
 W powders in a plastic capsule

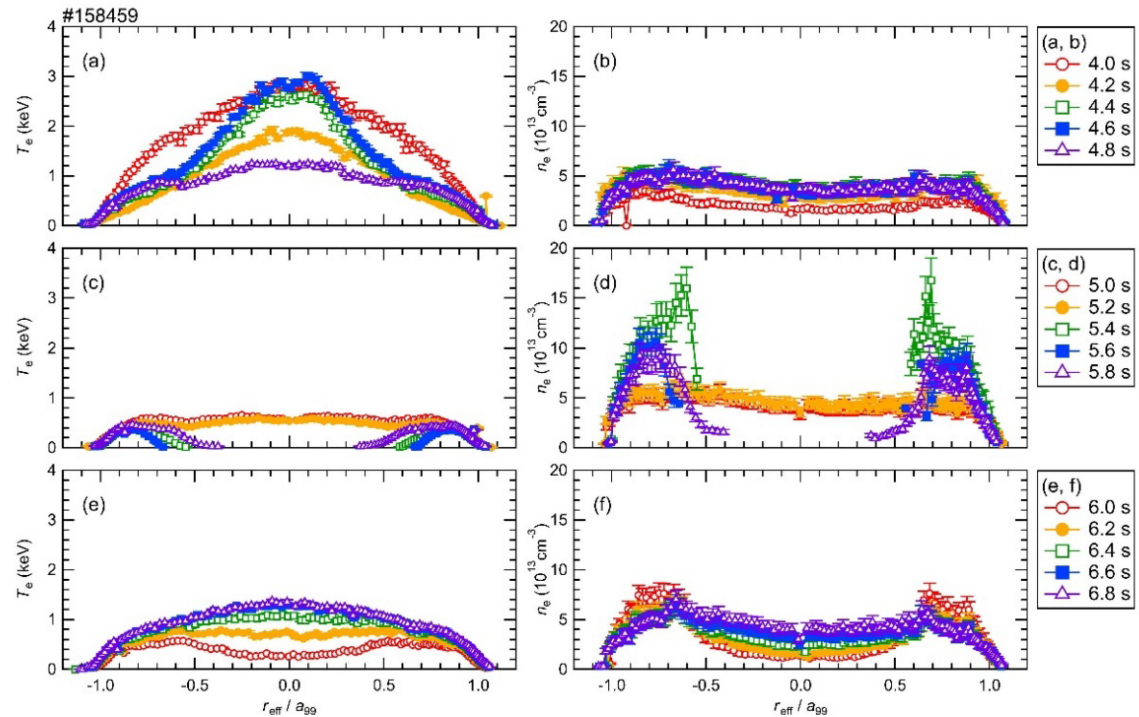
Two EUV spectrometers, EUV-Short (0.5-6 nm) and EUV-Long (10-50nm), and Visible and VUV spectrometers are equipped.

# 2.1 Examples of LHD experiments

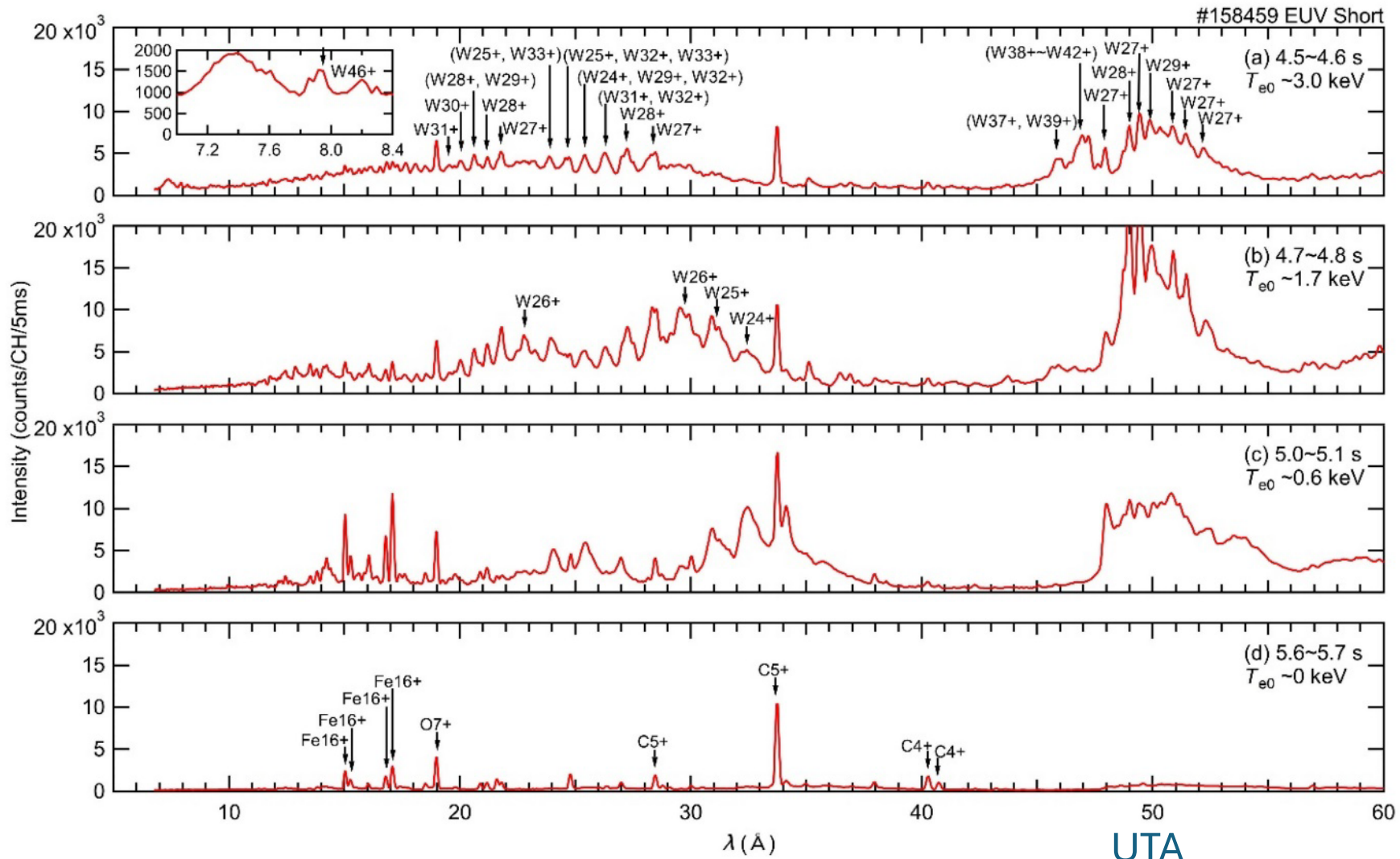
Oishi et al. *Atoms* **2021**, 9(3), 69



## Electron temperature and density distribution

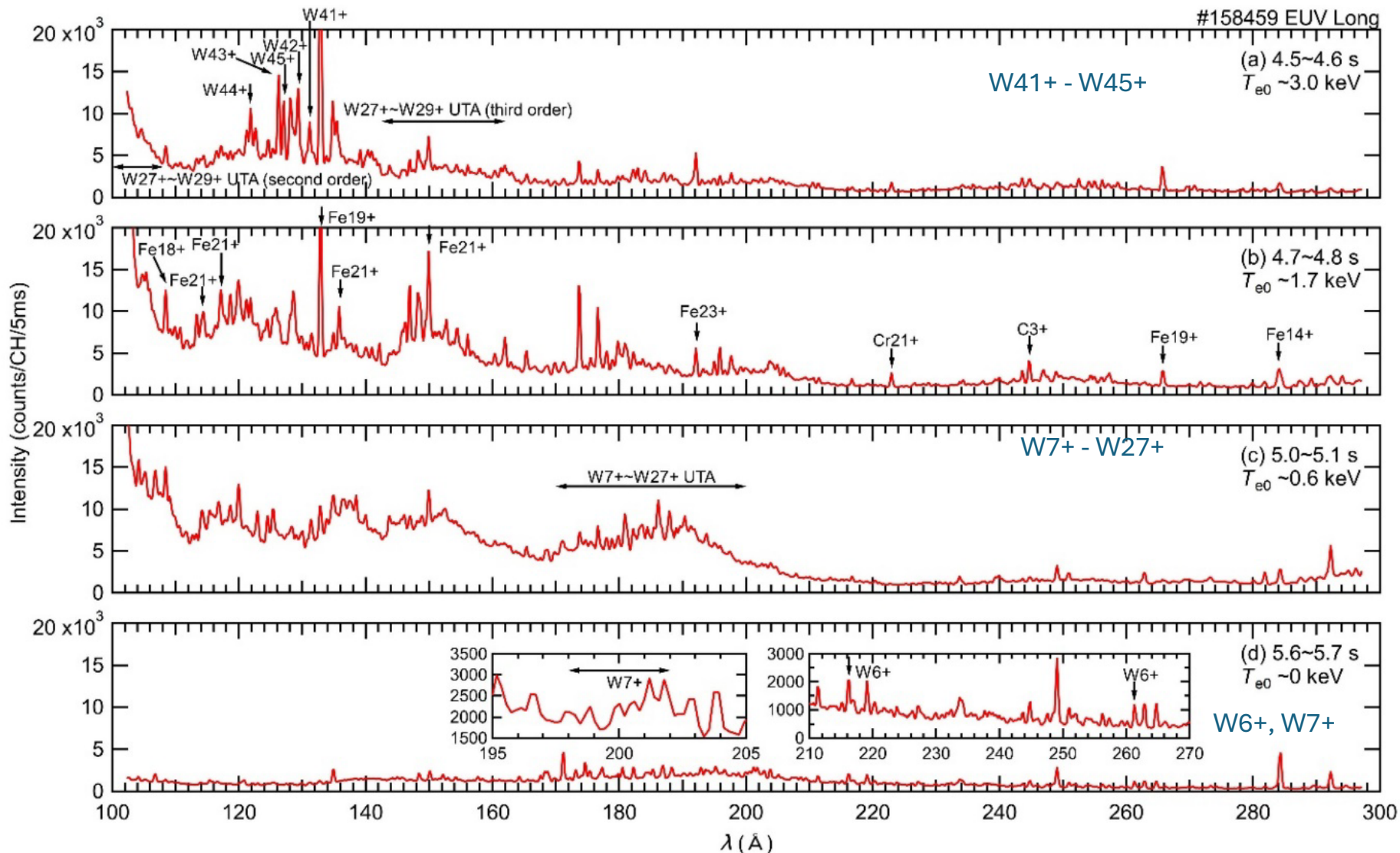


# 2.2 Soft X-ray / EUV spectra (0.7 -6 nm)

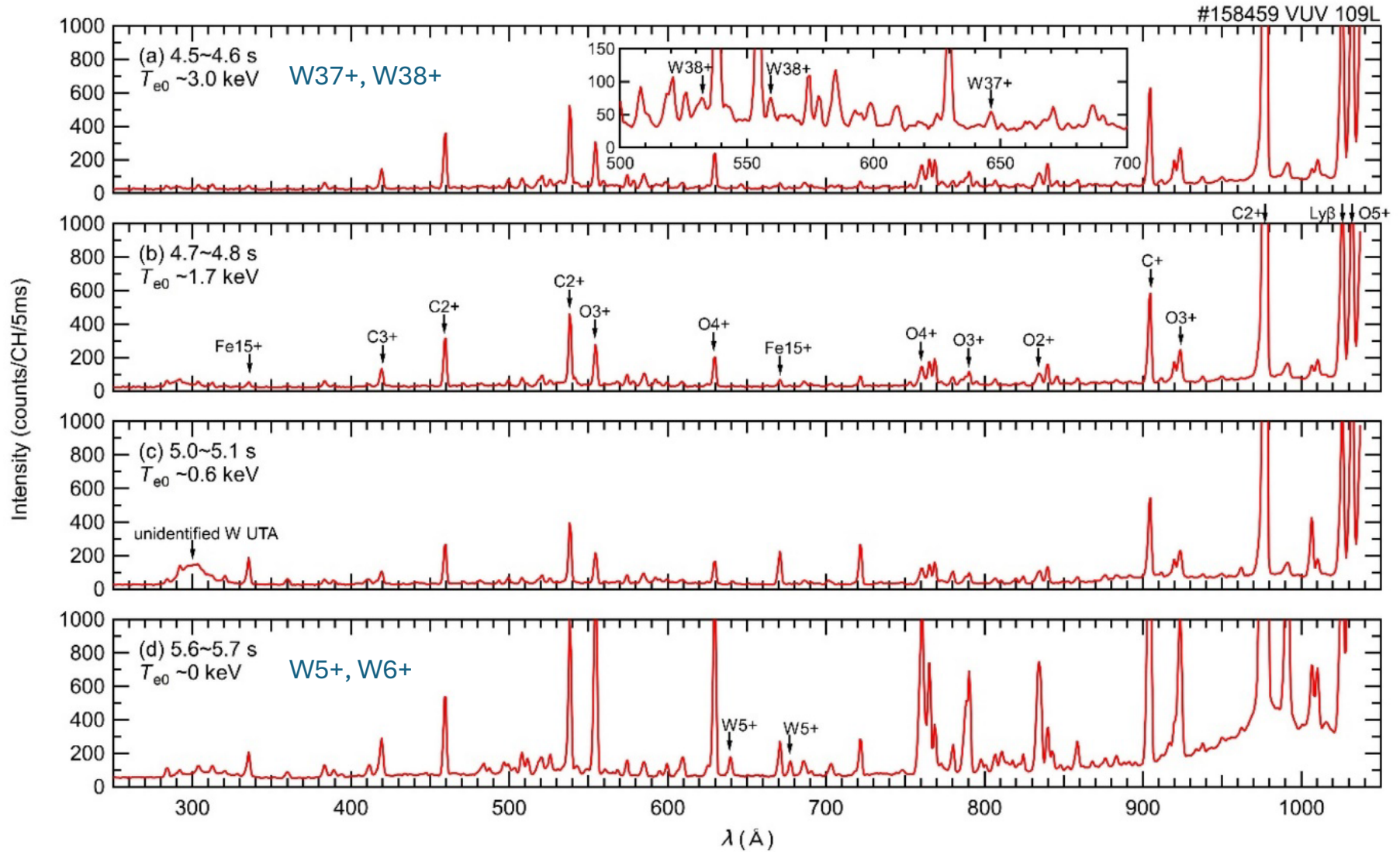


UTA  
W24+ - 42+  
W46+

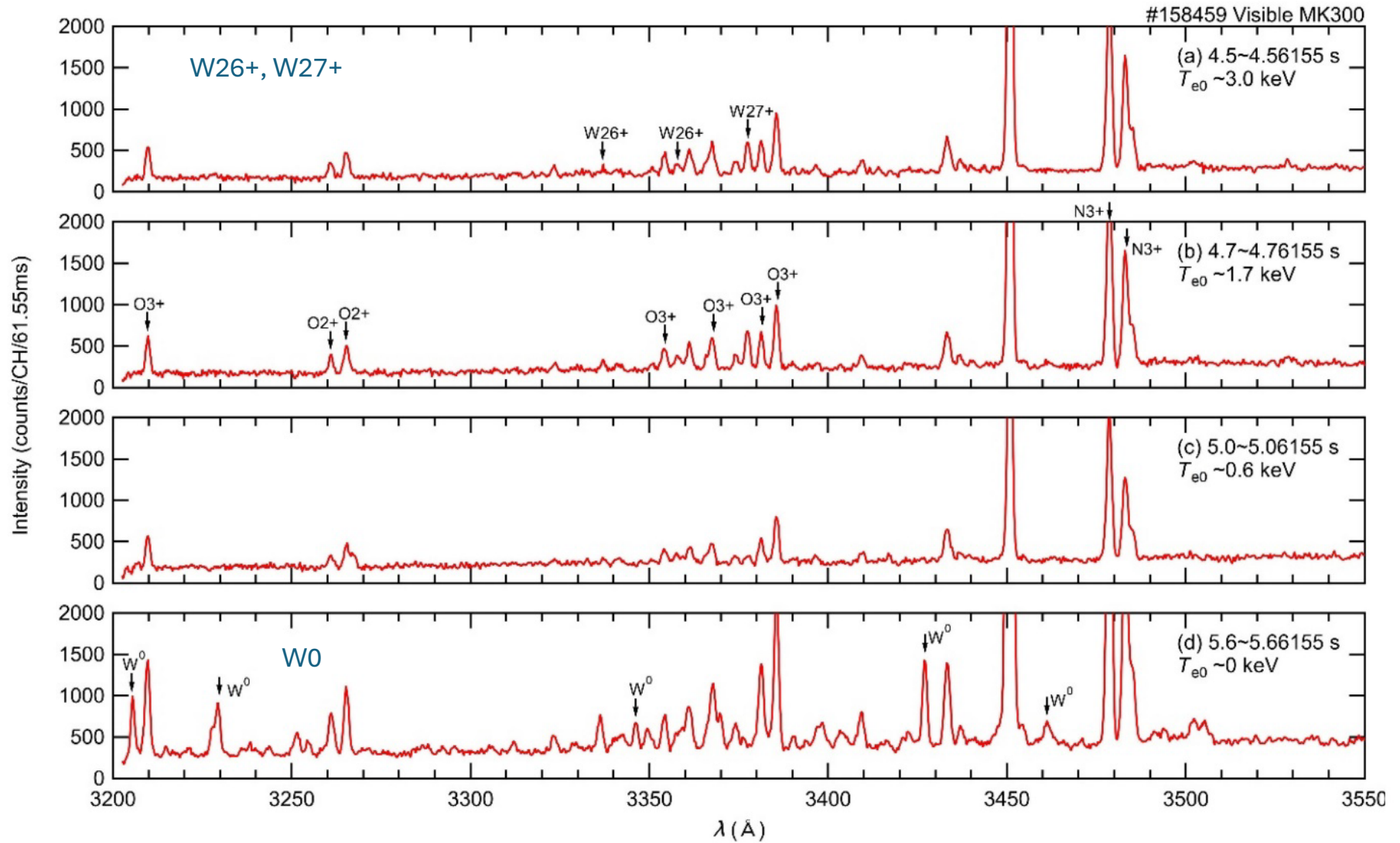
# 2.3 EUV spectra (10-30nm)



# 2.4 VUV spectra (25 – 105 nm)

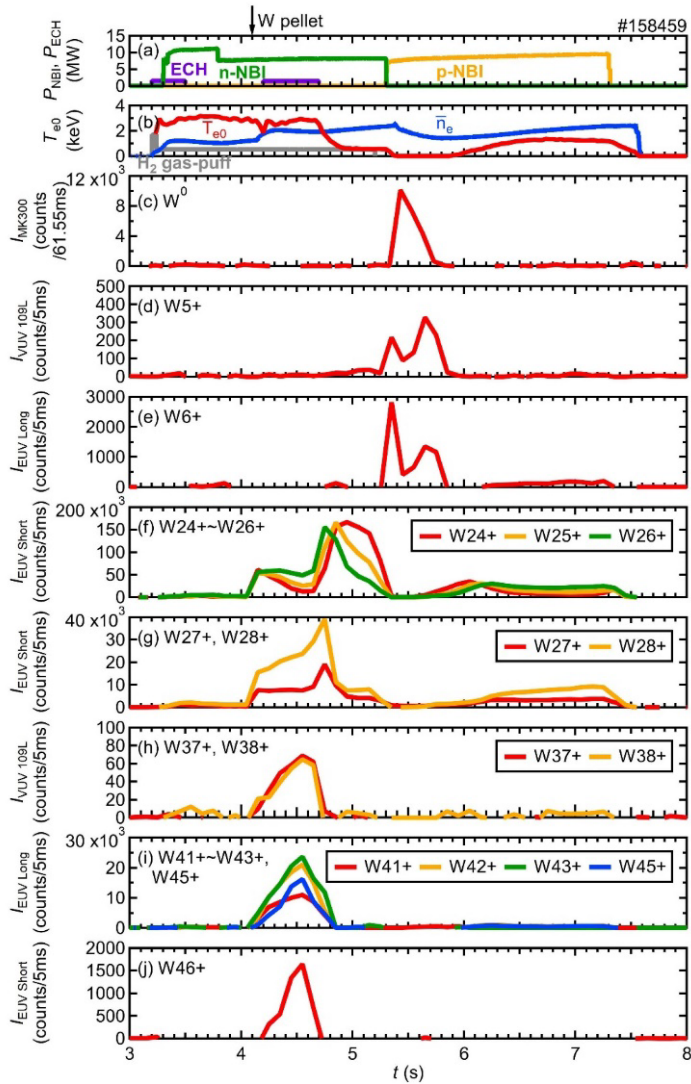


# 2.5 Visible spectra (320 – 355 nm)





# 2.7 Time evolution of W line intensities



3426.2–3427.9 Å for  $W^0$ ,

637.8–641.2 Å for  $W^{5+}$ ,

261.0–261.5 Å for  $W^{6+}$ ,

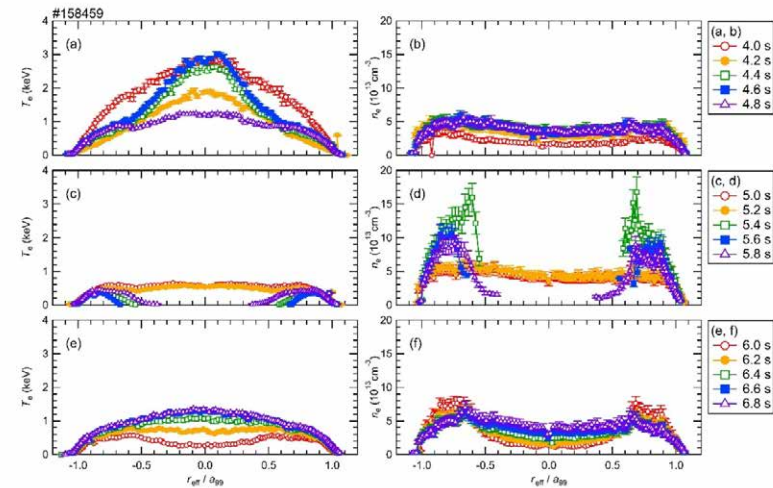
32.15–32.30 Å for  $W^{24+}$ , 30.73–31.69 Å for  $W^{25+}$ ,  
 29.29–30.40 Å for  $W^{26}$

28.58–28.69 Å for  $W^{27+}$ , 27.35–27.78 Å for  $W^{28+}$

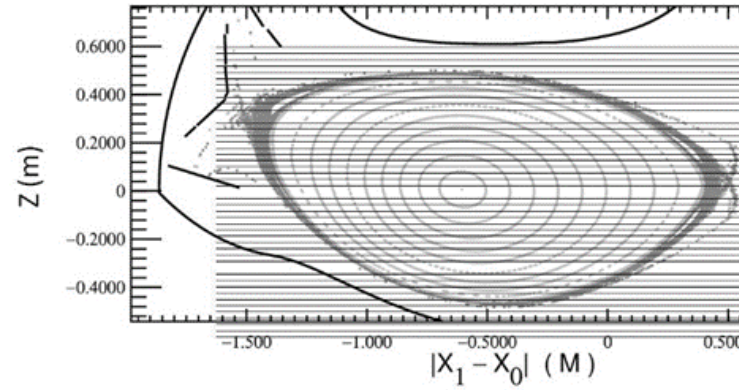
645.3–647.1 Å for  $W^{37+}$ , 558.6–560.3 Å for  $W^{38+}$

131.0–131.3 Å for  $W^{41+}$ , 129.2–129.5 Å for  $W^{42+}$ ,  
 126.1–126.5 Å for  $W^{43+}$ , 126.9–127.3 Å for  $W^{45+}$

7.89–7.95 Å for  $W^{46+}$ .



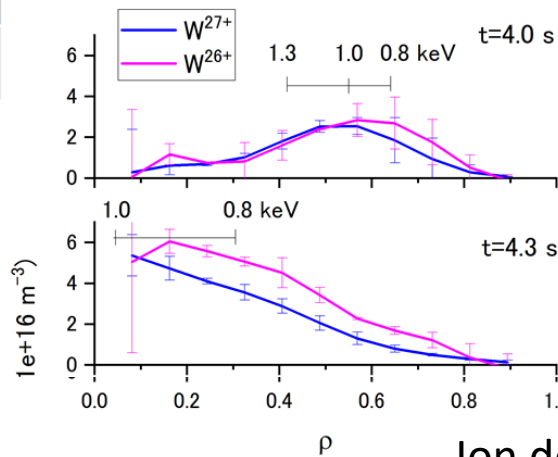
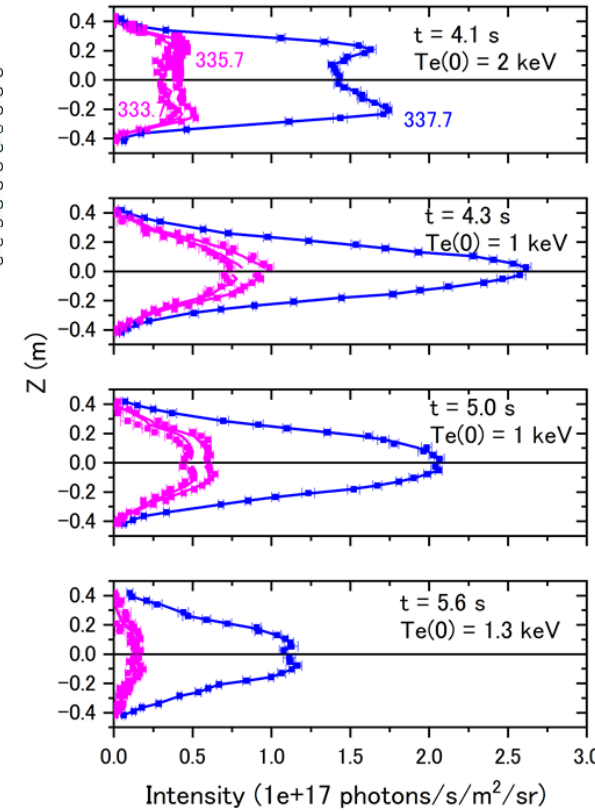
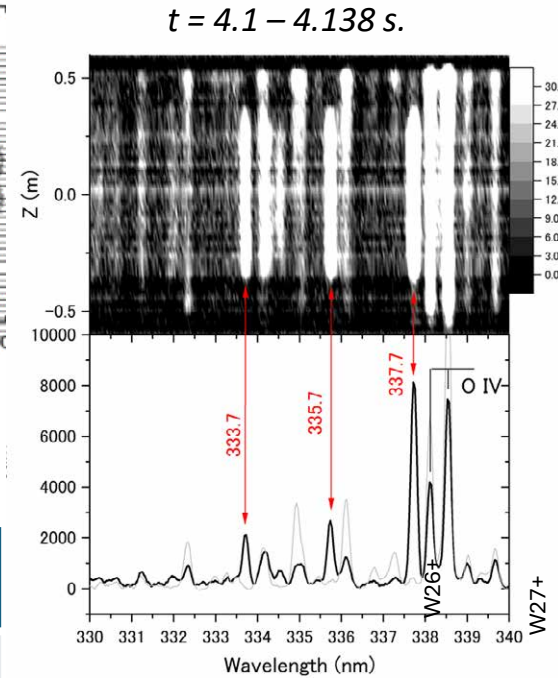
# 2.8 Visible M1 lines of $W^{26+}$ and $W^{27+}$ in LHD



- Visible M1 lines are used to examine W distribution in LHD plasmas.

q	Wavelength (nm)		Transition
	LHD	EBITs	
26	333.70(2)	333.748(9)	$(4f^2) \ ^3F_4 - ^3F_3$
26	335.73(2)	335.758(11)	$(4f^2) \ ^3F_4 - ^1G_4$
27	337.73(2)	337.743(26)	$(4f) \ ^2F_{7/2} - ^2F_{5/2}$

Visible lines are useful for diagnostics. M1 lines are measured and used to estimate ion densities in LHD.



Ion density distribution

# 2.9 Spatial distribution for EUV lines of $W^{24+}$ - $W^{26+}$

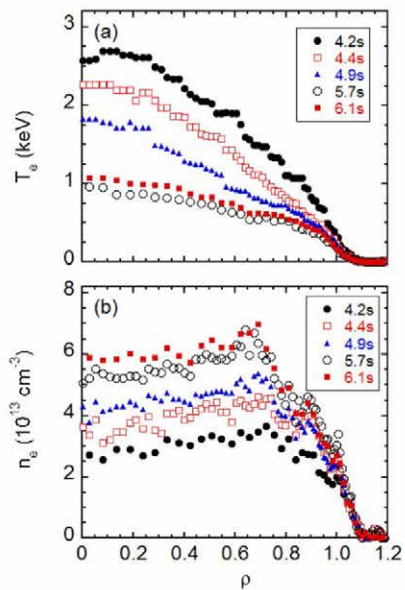


Fig. 3. (Color online) (a) Electron temperature and (b) density profiles at  $t = 4.2$  (just before pellet injection), 4.4 (just after pellet injection), 4.9, 5.7, and 6.1 s.

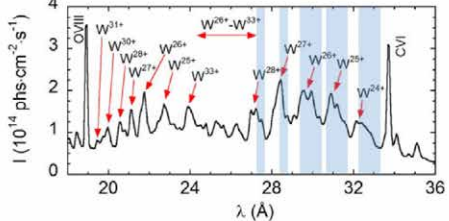


Fig. 4. (Color online) Tungsten UTA spectrum in wavelength range of 18–36 Å measured using EUV-Short. The shaded areas indicate wavelength intervals in which the UTA emission lines are composed of a single ionization stage.

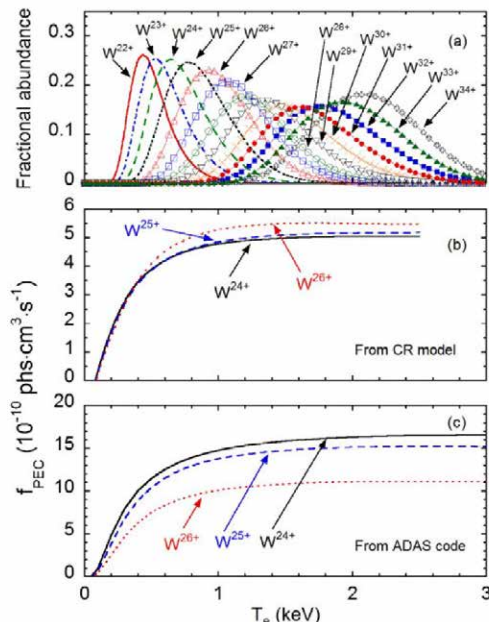
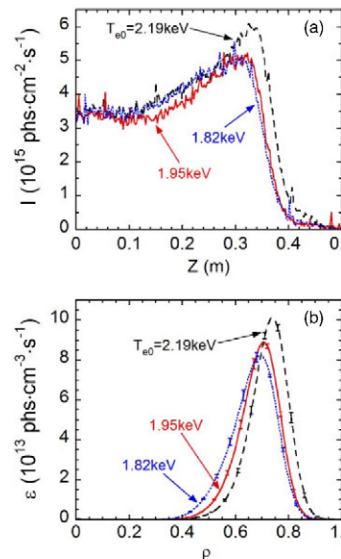


Fig. 5. (Color online) (a) Fractional abundance of  $W^{22+}$ – $W^{34+}$  calculated with ADAS code at  $n_e = 4 \times 10^{13} \text{ cm}^{-3}$ , and total photon emission coefficients of  $W^{24+}$  (32.16–33.32 Å; solid line),  $W^{25+}$  (30.69–31.71 Å; dashed line), and  $W^{26+}$  (29.47–30.47 Å; dotted line) calculated using (b) the present CR model and (c) ADAS code.



8. (Color online) (a) Vertical intensity and (b) local emission of  $W^{24+}$  at a wavelength interval of 32.16–33.32 Å plot rent central electron temperatures of  $T_{e0} = 2.19$  (dashed line), and 1.82 keV (dotted line).

Liu et al. (2018)

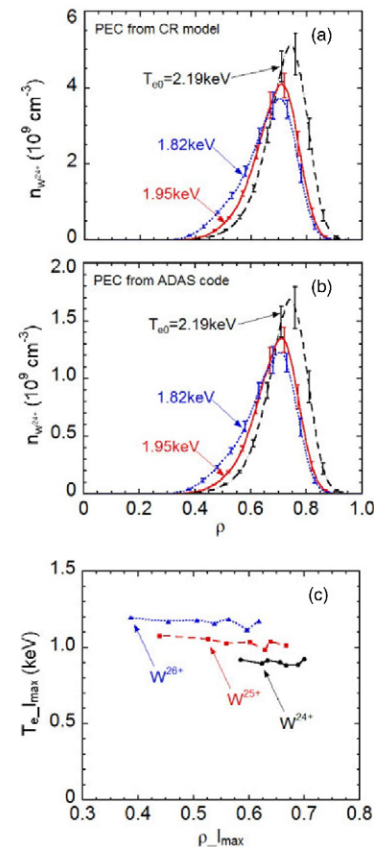


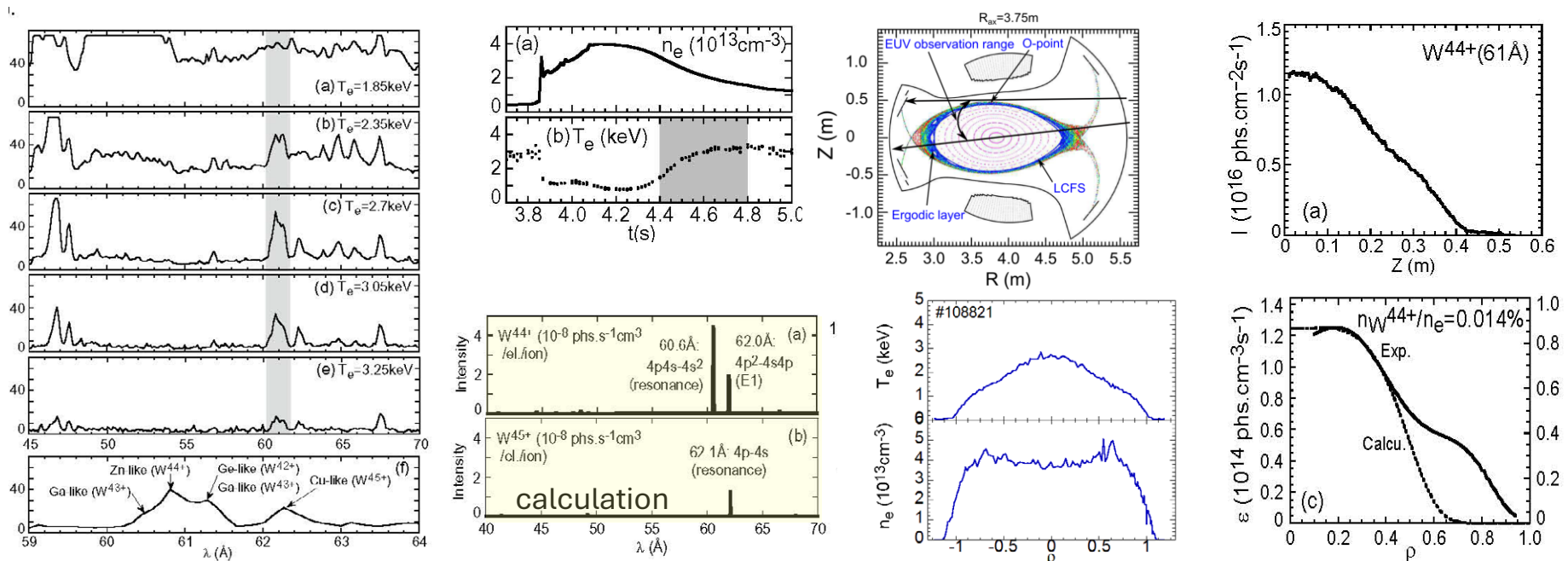
Fig. 9. (Color online) Density profiles of  $W^{24+}$  ions at  $T_{e0} = 2.19$  (dashed line), 1.95 (solid line), and 1.82 keV (dotted line) calculated using photon emission coefficient with (a) the present CR model and (b) ADAS code. (c) Electron temperature where the vertical intensity profiles of  $W^{24+}$  (32.16–33.32 Å),  $W^{25+}$  (30.69–31.71 Å), and  $W^{26+}$  (29.47–30.47 Å) take the maximum value as a function of normalized radius at the intensity maximum.

4f-5g transition UTA

# 2.10 Spatial profile of W<sup>44+</sup> ion

Morita et al. (2012)

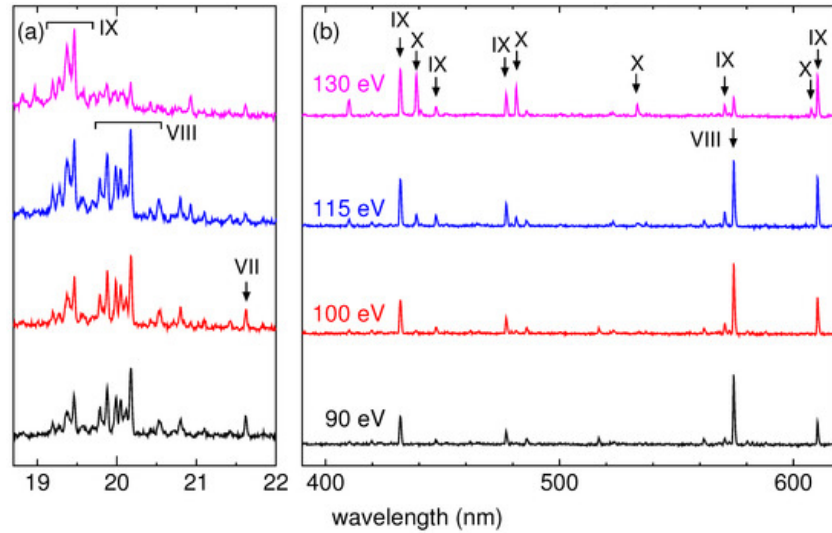
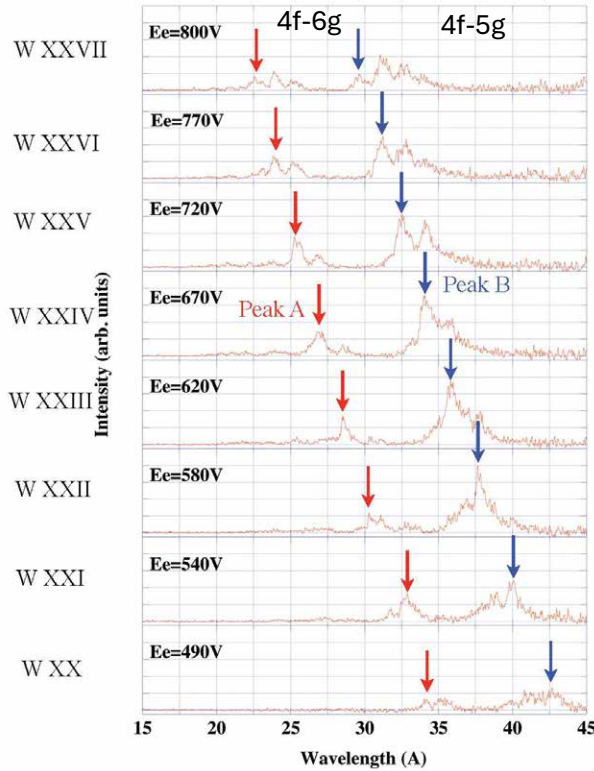
- Higher charged ions W<sup>42+</sup> -W<sup>45+</sup> were measured in the LHD at Te ~3keV.
- A radial profile of W<sup>44+</sup> ion was measured with 6.09nm (4s-4p transition) for the first time in LHD plasma.
- Emissivity coefficient of this transition is calculated with the CR model.
- Applying one-dimensional transfer model to the measured profile, centrally peaked emissivity profile of W<sup>44+</sup> ion is obtained (D=0.2m<sup>2</sup>/s, V=-1m/s is used)
- At the center, we obtained  $n(W^{44+})/n_e = 1.4 \times 10^{-4}$ . Total radiation power of tungsten is estimated as ~4MW. <-> NBI 8.2MW
- Tungsten is a dominant component of the radiation power.



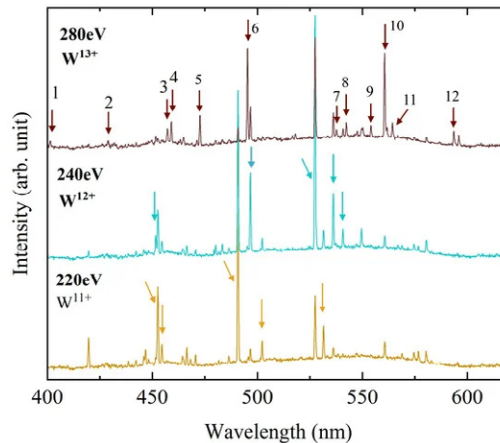
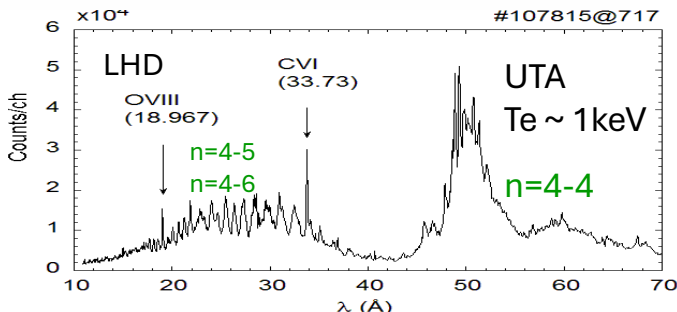
# 2.11 W spectra measured in EBIT

- EBIT has simpler plasma produced by mono-energy electron beam and is suitable to identify a charge state of spectral lines.

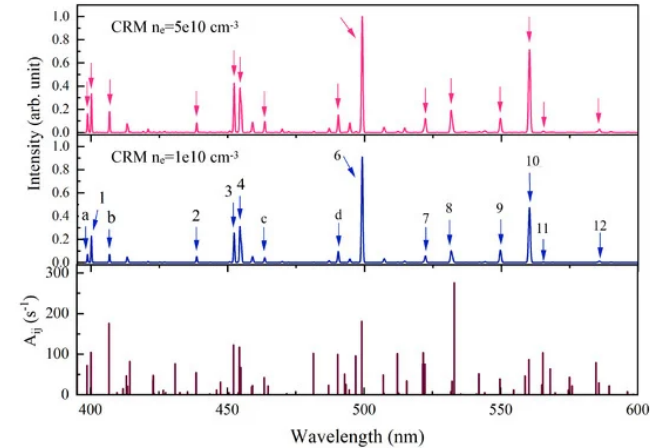
Sakaue et al. (2012)



Mita et al. (2017)



Priti et al. (2023)

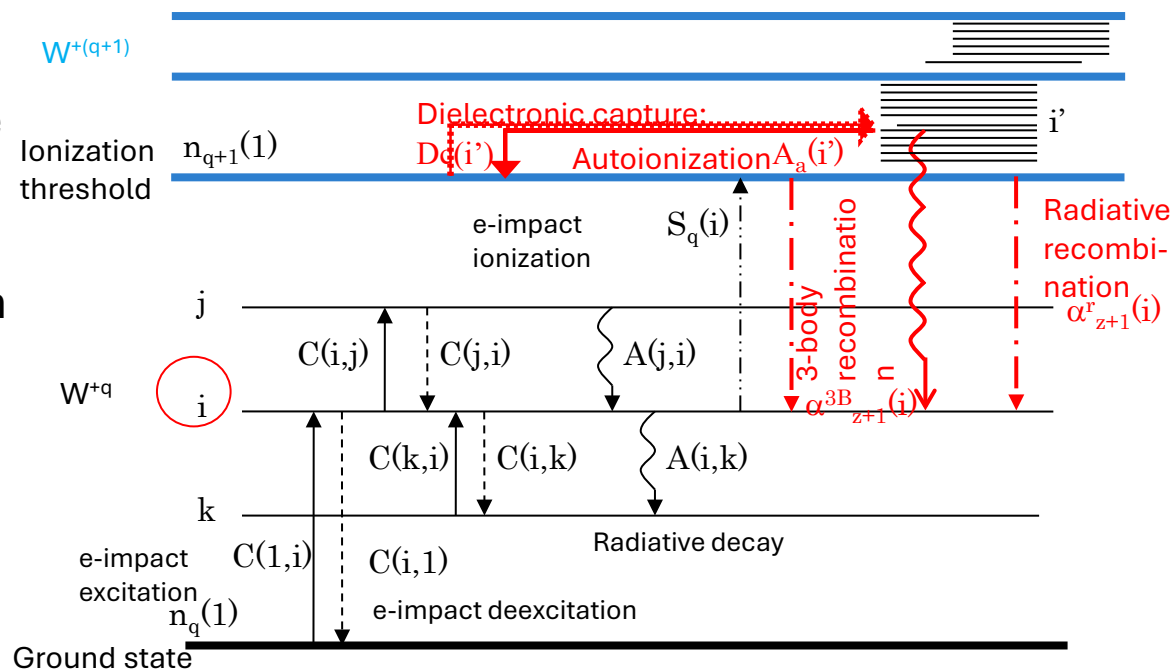


## 2.12 Requirements from the spectroscopy

- Good spectral lines to monitor tungsten ion behavior are needed for missing charge states  $q=7-12, 15-19, 30-36$ . So, the information on wavelengths, transitions, and intensities are needed from the theoretical calculations with CR models.
- For the transport study, evaluated ionization and recombination rates are required for all charge states.
- Line identification of visible lines are required. Many lines are found with EBIT experiments, but most of them are not identified with the transitions. Only charge states are estimated. So, precise detailed calculations on atomic structure are required.

# 3. Collisional-radiative model for W spectra

- CR model is to calculate population densities of excited levels under quasi-steady-state assumption.
- Atomic processes between excited states are considered in the rate equation for the population density of level  $i$ ,  $n_q(i)$ .
- Line intensity =  $A(i,j)n_q(i)\Delta E(i,j)$



$$\frac{dn_q(i)}{dt} = \Gamma_{in} - \Gamma_{out} = 0$$

Solution :  $n_q(i) = R_q^1(i)n_e n_q(1) + R_q^0(i)n_e n_{z+1}(1) + R_q^{CX}(i)n_H n_{z+1}(1)$

Ionizing plasma component and  
Recombining plasma component

Charge exchange with H atom could be important, but often ignored

$$\Gamma_{in} = \sum_{j<i} \{C(j,i)n_e n_q(j)\} + \sum_{k>i} \{F(k,i)n_e + A(k,i)\}n_q(k) + (Dc(i) + \alpha^r(i) + \alpha^{3B}(i)n_e)n_e n_{q+1}(1)$$

$$\Gamma_{out} = [S(i)n_e + S_{ai}(i) + \sum_{k>i} \{C(i,k)n_e\} + \sum_{j<i} \{F(i,j)n_e + A(i,j)\}]n_q(i)$$

# 3.1 Proton-impact excitation

- Proton-impact excitation plays important role for transitions between fine structure levels of the ground state, i.e. forbidden transitions like M1 which are measured in visible region.
- Intensities of M1 lines of  $W^{26+}$  (333.7 and 335.7nm) and  $W^{27+}$  (337.7nm) are affected by the proton-impact excitation and estimated ion density ratio is also affected.
- No data exists for the proton-impact excitation cross sections of tungsten ions.

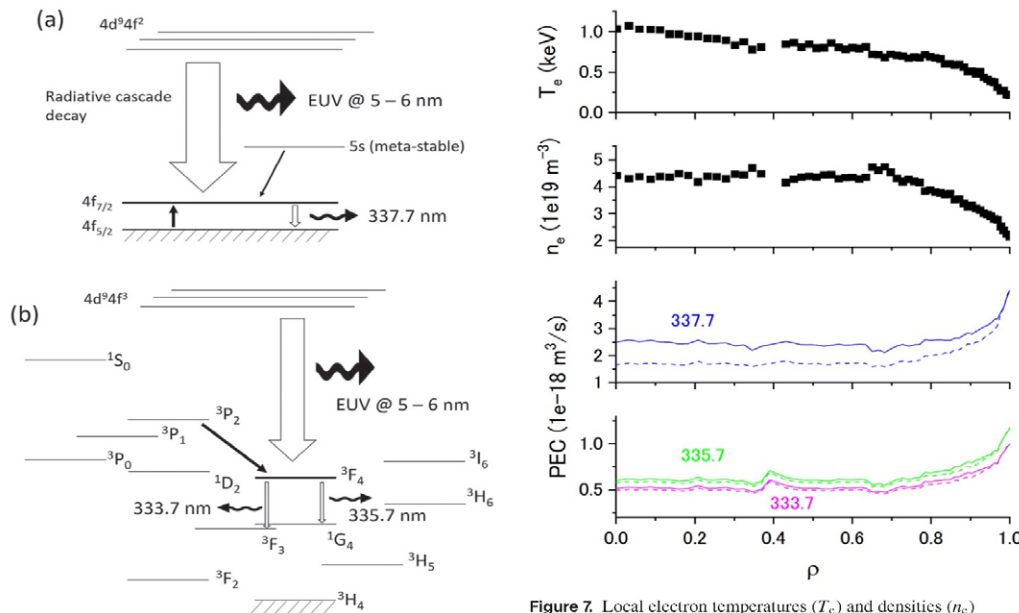


**Figure 6.** Schematic diagrams of M1 line emission for (a)  $W^{27+}$  (4f) and (b)  $W^{26+}$  ( $4f^2$ ). Solid and open arrows indicate population flows to the upper levels via collisional transition and radiative decay, respectively. Widths of the arrows represent magnitudes of the flow rates in the steady state.

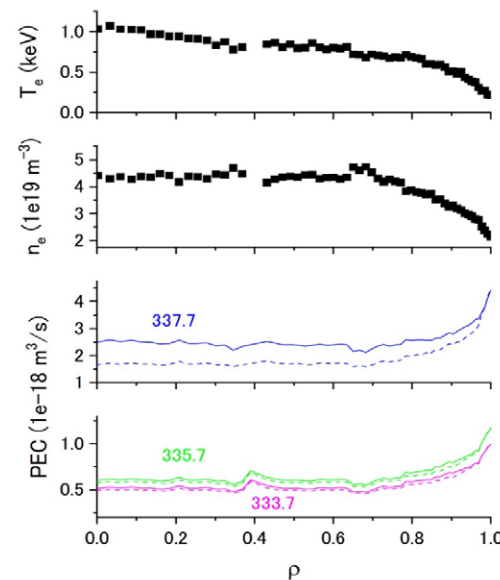
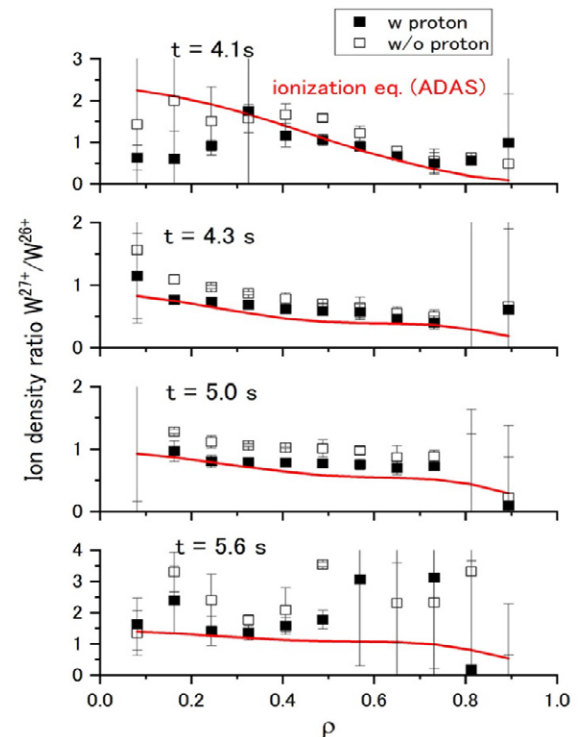


**Figure 7.** Local electron temperatures ( $T_e$ ) and densities ( $n_e$ ) measured by Thomson scattering as a function of the normalized minor radius  $\rho$  for  $t = 5.0$  s of the present discharge, and corresponding PECs of three M1 lines (solid lines). Dashed lines are the PECs without proton collision effects. Numbers are wavelengths (nm) of the M1 lines.

D. Kato et al. (2021) NF 61, 116008





## 3.2 Charge exchange with H atom

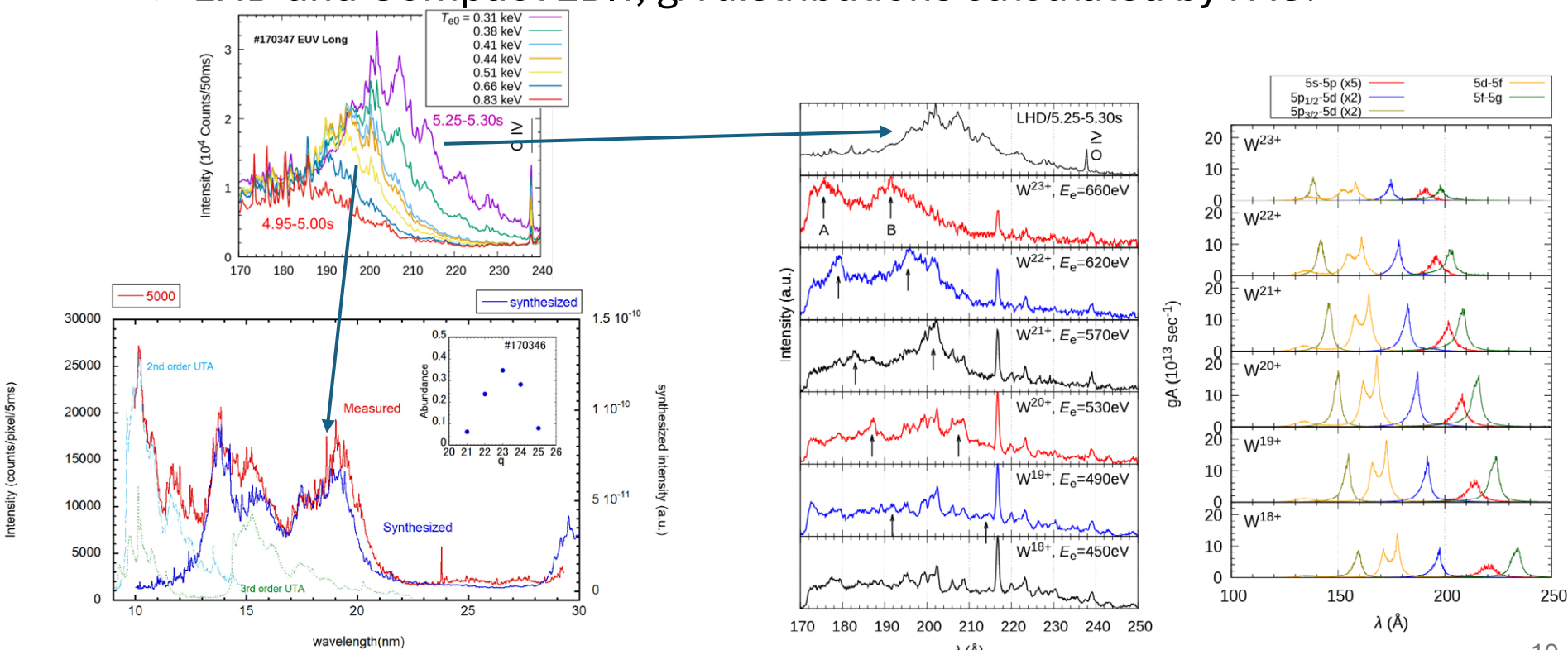
- Charge exchange process with H atom might change the ion densities and population densities, i.e. line intensities.
- Ralchenko et al. included CX process in their CR models with scaled (empirical) CX cross sections for  $W^{q+}$  ( $q=47-55$ ).
- Ralchenko and Schultz (PPCF 61 (2019) 125007) and Dipti et al. (PPCF 63 (2021) 115010) examined charge exchange recombination spectroscopy of  $W^{q+}$  ( $q=61-66$ ) using CX cross sections calculated with CTMC methods. No work for other charge states.
- There are difficulties in CX cross section calculations for many electron systems, e.g. CTMC, AO, MO methods etc.
- It is also difficult to measure CX cross sections with W ions and H atoms.
- Data are needed.

## 3.3 Atomic data for CR models

- In order to construct a CR model, large set of atomic data are needed for highly charged tungsten ions. Especially to explain UTA feature, large number of energy levels should be considered in the CR model. It is difficult to evaluate such large set of atomic data themselves. Comparison with measured spectra is the only way to check the calculation.
  - Are there any methods?
  - How to open atomic data or CR model for applications?
  - Cross check with other atomic data and/or CR models?
- $W^{q+}$  with  $q < 21$  ( $4d^{10}4f^a$ ,  $a > 7$ ) have many fine structure levels. Calculations of atomic data and CR model take long time. Are there any good methods / approximations? I am trying to construct CR models for  $W^{19+}$  and  $W^{18+}$ .

# 3.4 W ions spectra with $T_e < 1\text{keV}$

- Murakami et al. (IAEA TM 2023)
  - $W^{q+}$   $q=21-25$ , EUV 10-30nm measured in LHD. UTA ( $n=5-5$ )
  - CR model with atomic data calculated by HULLAC. Recombination processes are included.
- Nishimura et al. Plasma Fusion Res. 19, 1402022 (2024)
  - $W^{q+}$ ,  $q=18-23$ , EUV ( $\sim 20\text{nm}$ )
  - LHD and Compact EBIT, gA distributions calculated by FAC.



Murakami et al. (2023, IAEA TM)

Nishimura et al. (2024)

## 4. Summary

- We have large number of tungsten spectra measured in LHD plasmas from soft X-ray to visible range. We identified useful lines to examine tungsten behavior in magnetically confined plasmas, but lines for  $W^{q+}$   $q=7-12$ ,  $15-19$ ,  $30-36$  are not well identified yet.
- Visible lines should be identified for monitoring reactor plasma for future.
- Reliable ionization and recombination rate coefficients for all charge states are to be set after evaluation.
- Proton-impact excitation cross sections are needed.
- Charge exchange cross sections for H-W ion collisions are needed.
- CR models with many levels are needed for  $q < 20$ .
- Note: LHD will be shutdown at the end of 2025. Compact Helical System (CHS) will be used for plasma experiments in 2026. We have a plan to make a new EBIT at NIFS, which will work in 2027.